Journal of Theoretical Biology 575 (2023) 111646

Contents lists available at ScienceDirect

Journal of Theoretical Biology

journal homepage: www.elsevier.com/locate/yjtbi

A mathematical model of cell movement and clustering due to chemotaxis

Adam Farmer, Paul J. Harris *

School of Architecture, Technology and Engineering, University of Brighton, Brighton, UK
Centre for Regenerative Medicine and Devices, University of Brighton, Brighton, UK

ARTICLE INFO

Keywords:
Chemotaxis
Mathematical modelling
Cell migration
Cell clustering

ABSTRACT

This paper presents a numerical method for modelling cell migration and aggregation due to chemotaxis where the cell is attracted towards the direction in which the concentration of a chemical signal is increasing. In the model presented here, each cell is represented by a system of springs connected together at node points on the cell's membrane and on the boundary of the cell's nucleus. The nodes located on a cell's membrane are subject to a force which is proportional to the gradient of the concentration of the chemical signal which mimics the behaviour of the chemical receptors in the cell's membrane. In particular, the model developed here will consider what happens when two (or more) cells collide and how their membranes connect to each other to form clusters of cells. The methods described in this paper will be illustrated with a number of typical examples simulating cells moving in response to a chemical signal and how they combine to form clusters.

1. Introduction

A typical cell consists of an outer membrane which encloses the cytoplasm that makes up the majority of the interior of the cell. The nucleus of the cell is located within the cytoplasm and is a lot stiffer than the cytoplasm. This means that the cytoplasm will deform more than nucleus. Moreover, the size of the nucleus has an impact on the cell displacement, and a cell will move further when the nucleus is smaller (Hervas-Raluy et al., 2019).

The shape and size of the part of the cell membrane that forms the leading edge of a cell that is reacting to a chemical signal has a significant effect on the motion of the cell. Further, changes in the cell shape due to migration or deformation in response to a signal are known to have an impact on the shape and location of the nucleus inside the cell (Ben-David and Weihs, 2021). Therefore, to be able to efficiently model the cell, we need to develop a system of equations to model the motion of both the membrane and the nucleus, and how the motion of one affects the motion of the other.

Cell invasion is a crucial step in the process of metastasis formation which leads to the often lethal spread of cancer in the body (Ben-David and Weihs, 2021). Cell invasion requires the cell's cytoskeleton to remodel in order to account for dynamic changes and applied forces. During the invasion process, the cells squeeze through dense tissues to migrate to the desired site. The cytoskeleton can be dynamically generated, restructured and concentrated at specific locations to facilitate force application where it is advantageous to do so (Alvarez-Elizondo et al., 2021; Ben-David and Weihs, 2021). When considering cancer cells, it has been shown that they apply stronger adhesive and traction forces when compared to benign cells, and that they also are stiffer and maintain their shape more during migration (Ben-David and Weihs, 2021; Massalha and Weihs, 2017). The ability of cells to change shape, modify their internal structure (cytoskeleton and nucleus) and alter adhesion and migratory states is directly correlated with their ability to invade surrounding tissue (Massalha and Weihs, 2017).

Lamellipodia are tentacle like structures that drive cell migration. These structures reach out and probe the environment so that they can attach to another cell, and help draw the cell in closer and promote movement. The motion of a typical group of cells is shown in Fig. 1. The cells which are on the right of the image can be seen to form a lamellipodia towards the cells on the left which provides a mechanism for the cells to come together and form a cluster. Once the cells have collided they can adhere to each other by physically attaching their cell membranes using surface proteins like cadherins.

It is well-known that a cell can be guided by different stimuli such as mechanotaxis, thermotaxis, chemotaxis and/or electrotaxis (Mousavi and Doweidar, 2015). Since chemotaxis and mechanotaxis are the most common causes of cell motion (Peng and Vermolen, 2020) they are the ones that will be considered in this paper.

Chemotaxis is the process where cells move in response to chemical signals in their environment (Mousavi and Doweidar, 2015). These signals are usually in the form of proteins that can stimulate receptors in the cells outer membrane and cause the membrane to extend in the direction in which the concentration of the signal is increasing, often

* Corresponding author at: School of Architecture, Technology and Engineering University of Brighton, Brighton, UK.
E-mail address: p.j.harris@brighton.ac.uk (P.J. Harris).

https://doi.org/10.1016/j.jtbi.2023.111646
Received 24 October 2022; Received in revised form 10 August 2023; Accepted 12 October 2023
Available online 16 October 2023

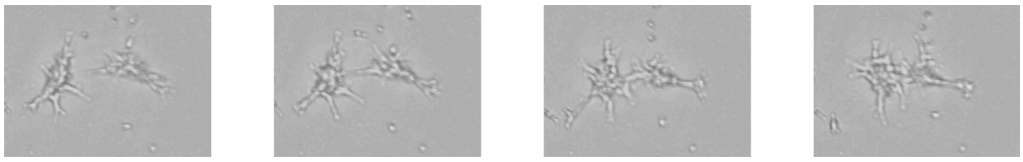

Fig. 1. Still images taken from a time-lapse video showing the development of lamellipodia from the cells on the right and how the resulting motion of the cells cause them to come together to form a small cluster. Images courtesy of the Brighton Center for Regenerative Medicine and Devices.

forming lamellipodia. In some cases the chemical signal, with a known concentration gradient, simply exists in the environment containing the cells. However, in other cases the chemical signal may secreted by a cell in order to attract other nearby cells to form clusters of cells, and it is the latter case that we concerned about in this paper. Typically a cell will emit a burst of the protein that is the chemical signal and this will spread into the surrounding environment, often via a diffusion type process.

Mechanotaxis is the movement of a cell and/or deformation of the shape of a cell due to a mechanical process, such as when one cell collides with another cell. When two cells collide the sections of their membranes that are in contact will adhere to each other and deform so that the forces across parts of the membrane that are in contact are in equilibrium.

The shape of a cluster (or clusters) of cells obtained by chemotaxis and mechanotaxis will depend on the initial locations of the cells involved. Conversely, it may be desirable to determine the initial locations of the cells which leads to the formation of a cluster which has a particular shape. The number of laboratory experiments that would be needed to determine the initial locations of the cells which ultimately form a cluster with the desired shape could be very large and so would be costly and extremely time consuming to carry out. An alternative is to use a mathematical/computational model which can simulate the shape of the cluster (or clusters) obtained from a given initial configuration relatively quickly, and so can be used to analyse a large number of initial configurations in much less time than is possible with experiments, and at almost zero financial cost. In this paper we present a mathematical/computational method for determining the shape of the cluster (or clusters) formed through chemotaxis and mechanotaxis for cells which can be in any initial configuration.

We have two choices for the type of model that we use to simulate the motion of cells: Particle models or cell-based models. In particle based models the cells are represented by simple geometric shapes such as in the models proposed by Eyiyurekli et al. (2008), Thompson et al. (2012) and Kim et al. (2014) for example. Harris (2017) has developed a particle based model of how small clusters of cells combine to form larger clusters. Whilst there is some experimental evidence that the cells can be treated as rigid particles as they move (see the images in Nitta et al. (2007) for example) there is a growing body of experimental evidence that the cells change shape as they move, as shown in Fig. 1. However, the advantage of particle based models is that they are computationally cheap and can model the motion of thousands of individual cells relatively quickly (Harris, 2017).

The alternative is to use cell based models where the changes in the shape of each cell in response to a chemical signal and/or colliding with its neighbours is simulated. Elliott et al. (2012) developed a finite element model of a cell moving in response to a chemical signal. However, the methods proposed in Elliott et al. (2012) would be computationally expensive to apply to situations with a large number of cells.

Sfakianakis et al. (2018) and Löbor et al. (2015) developed models where cells move in close vicinity to each other using a system of potentials to model the attractive and repulsive forces between the cells. However, their simulations do not include cells connecting together and forming clusters.

A method based on representing a cell as a system of springs has been proposed in Vermolen (2015) and Chen et al. (2018). In these

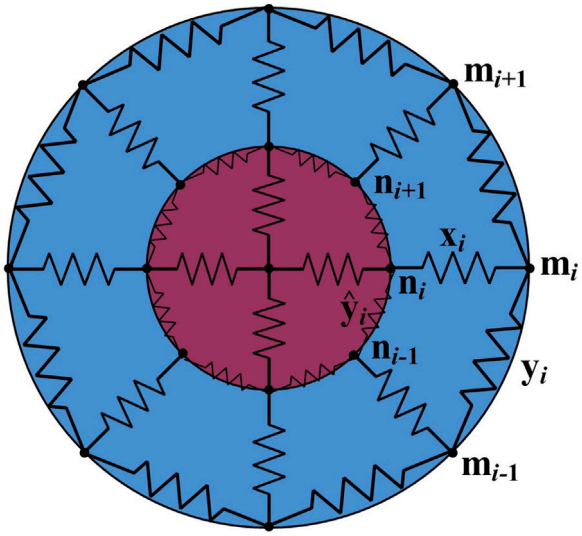

Fig. 2. An illustration of the nodal points on the cell boundary membrane and surface of the nucleus. The cytoskeleton is represented as a collection of springs.

model the nodes on a cells membrane detect and move in response to the chemical signal deforming the cell. The interior of the cell then moves in order to keep the forces due to the springs in equilibrium. In addition, if the chemical decays and disappears, the spring-based model ensures that the cells will return to their original shape provided that they have not collided. It is this model that we shall use as the basis for our model of cell collisions.

In Section 2 we will introduce our model using a spring system to represent the deformations of each cell. In Sections 2.1 and 2.2 we introduce the differential equations that describe the deformations of the cell membrane and nucleus respectively. Sections 2.3 and 2.4 describe how the centre of mass of each cell is calculated and how we model the spread of the chemical signal respectively. How cell collisions are detected, and how the differential equations need to be modified to account for the cells now being connected, is discussed in Section 2.5. Finally, in Section 2.6 we describe the time-stepping scheme used here. The methods described in this paper are illustrated for a number of typical examples in Section 3.

2. Mathematical model

Let $\mathbf{m}_i$ be the position of the ith nodal point on the cell membrane, $\mathbf{n}_i$ be the position of the ith nodal point on the nucleus, and $\mathbf{c}$ be the position of the centre of the nucleus, as shown in Fig. 2. Let $\mathbf{x}_i$ be the original position vector of $\mathbf{n}_i$ relative to $\mathbf{m}_i$ (that is, $\mathbf{x}_i = \mathbf{n}_i - \mathbf{m}_i$ when $t = 0$) and similarly let $\hat{\mathbf{x}}_i$ be the original position vector of $\mathbf{n}_i$ relative to $\mathbf{c}$.

In the model presented here the nodes are consecutively numbered around the membrane and the boundary of the nucleus in an anticlockwise direction starting at the positive x-axis. It is noted that both the cell membrane and the boundary of its nucleus are closed curves and so the first and last nodes on both curves will be adjacent to each other.

This means that if there are N nodes on the cell membrane then when deriving the equations for the first and last nodes on the membrane we have $\mathbf{m}_{-1} = \mathbf{m}_N$ and $\mathbf{m}_{N+1} = \mathbf{m}_1$. Similarly if there are N nodes on the boundary of the nucleus then $\mathbf{n}_{-1} = \mathbf{n}_N$ and $\mathbf{n}_{N+1} = \mathbf{n}_1$. This needs to be taken into account when substituting $i = 1$ and $i = N$ into the general equations derived in the sections below.

2.1. Forces acting on nodes on the membrane

Consider the forces acting on a nodal point on the cell membrane. There are a number of different forces acting on each node on the membrane and we shall consider each of these in turn.

The nodal points on the membrane can detect and react to the gradient of an incoming signal. This can be accounted for this in the equations by having a force proportional to the gradient of the concentrations acting on each node on the membrane. Thus the first contribution to the force on a node on the membrane is

$$d\mathbf{m}_i(t) = \beta \nabla c(t, \mathbf{m}_i(t))\, dt \tag{1}$$

where $\nabla c(t, \mathbf{m}_i(t))$ is the gradient of the signal concentration and the variable β is used to control the magnitude of the cells response to external stimuli and helps to define how sensitive the cell is to the concentration gradient. The concentration of the chemical signal is discussed in Section 2.4.

The model also needs to account for the forces due to the motion of the nodes that are adjacent to the current node. The extension or compression of the spring that represents the connection between $\mathbf{n}_i(t)$ and $\mathbf{m}_i(t)$ can be expressed as

$$\mathbf{n}_i(t) - \mathbf{m}_i(t) - \mathbf{x}_i$$

where $\mathbf{x}_i$ is the original position vector of $\mathbf{n}_i$ relative to $\mathbf{m}_i$ when $t = 0$. That is, $\mathbf{x}_i = \mathbf{n}_i(0) - \mathbf{m}_i(0)$. Introducing the parameter α, the Internal Cell Membranes Relaxation Coefficient, we can vary how stiff the cytoskeleton is and how deformed the cell can get. This is analogous to the stiffness of a spring. Hence the second contribution to the equation of motion of the ith node on the membrane is

$$d\mathbf{m}_i(t) = \alpha(\mathbf{n}_i(t) - \mathbf{m}_i(t) - \mathbf{x}_i)\, dt \tag{2}$$

We also need to account for the changing relative position of the adjacent nodal points on the membrane by including springs between nodal points on the cell's membrane. For this, we introduce a new parameter δ, which is the External Cell Membranes Relaxation Coefficient. The extension (or compression) of the spring that represents the connection between $\mathbf{m}_i(t)$, $\mathbf{m}_{i+1}(t)$ (which is the next nodal point from i in a clockwise direction), and $\mathbf{m}_{i-1}(t)$, (which is the next nodal point from i in the counter-clockwise direction). Let $\mathbf{y}_i$ denote the original position vector of $\mathbf{m}_i$ relative to $\mathbf{m}_{i-1}$ (so $\mathbf{y}_i = \mathbf{m}_i(0) - \mathbf{m}_{i-1}(0)$). At time t the compression or tension of the springs connecting the i^{th} node to the adjacent nodes is given by

$$\mathbf{y}_i - (\mathbf{m}_{i-1} - \mathbf{m}_i) - \mathbf{y}_{i+1} + (\mathbf{m}_i - \mathbf{m}_{i+1}).$$

Hence the contribution to the force acting on the ith node is

$$d\mathbf{m}_i(t) = \delta \left[\mathbf{y}_i - (\mathbf{m}_{i-1} - \mathbf{m}_i) - \mathbf{y}_{i+1} + (\mathbf{m}_i - \mathbf{m}_{i+1})\right]\, dt. \tag{3}$$

Summing the contributions given by (1), (2) and (3) gives the total force acting on the ith node on the membrane as

$$\begin{aligned} d\mathbf{m}_i(t) \quad = \quad & \beta \nabla c(t, \mathbf{m}_i(t)) dt \\ & + \alpha(\mathbf{n}_i(t) - \mathbf{m}_i(t) - \mathbf{x}_i) dt \\ & + \delta \left[\mathbf{y}_i - (\mathbf{m}_{i-1} - \mathbf{m}_i) - \mathbf{y}_{i+1} + (\mathbf{m}_i - \mathbf{m}_{i+1})\right]\, dt. \end{aligned} \tag{4}$$

2.2. Forces acting on nodes on the nucleus

Each node on the boundary of the nucleus will interact with the corresponding node on the membrane, the node at the centre of the cell and the two nodes on the boundary on the nucleus that are either side of the current node. Recall that $\mathbf{n}_i$ is the location of the ith node on the boundary on the nucleus, and $\mathbf{c}$ is the location of the centre of the nucleus. Following a similar analysis to that carried out above for nodes on the membrane, we obtain

$$\begin{aligned} d\mathbf{n}_i(t) \quad = \quad & \alpha_n(\mathbf{c}(t) - \mathbf{n}_i(t) - \hat{\mathbf{x}}_i) dt \\ & - \alpha(\mathbf{n}_i(t) - \mathbf{m}_i(t) - \mathbf{x}_i) dt \\ & + \delta_n \left[\hat{\mathbf{y}}_i - (\mathbf{n}_{i-1} - \mathbf{n}_i) - \hat{\mathbf{y}}_{i+1} + (\mathbf{n}_i - \mathbf{n}_{i+1})\right]\, dt. \end{aligned} \tag{5}$$

where α_n and δ_n are the Internal Nucleus Relaxation Coefficient and Nucleus Boundary Relaxation coefficient respectively; $\hat{\mathbf{x}}_i$ is the position vector of $\mathbf{n}_i$ relative to $\mathbf{c}$ when $t = 0$ and $\hat{\mathbf{y}}_i$ is the position vector of $\mathbf{n}_i$ relative to $\mathbf{n}_{i-1}$ when $t = 0$.

2.3. Centre of mass

To accurately model the cell, we need to account for the movement of the centre of mass of the cell. Here the shape of both the outer membrane of the cell and its nucleus are represented by the polygons that are obtained by connecting the nodes on each boundary by straight lines. Then the centre of mass of the cell $\mathbf{c} = (\bar{x}, \bar{y})^T$ is given by

$$\bar{x} = \frac{M_x}{A}, \quad \bar{y} = \frac{M_y}{A}$$

where

$$\begin{aligned} M_x \quad = \quad & \frac{\rho_1}{6} \sum_{i=1}^{N} [(x_i - x_{i+1})[(y_i + 2y_{i+1})x_{i+1} + (2y_i + y_{i+1})x_i]] \\ & + \frac{\rho_2 - \rho_1}{6} \sum_{i=1}^{N} [(\hat{x}_i - \hat{x}_{i+1})[(\hat{y}_i + 2\hat{y}_{i+1})\hat{x}_{i+1} + (2\hat{y}_i + \hat{y}_{i+1})\hat{x}_i]] \\ M_y \quad = \quad & \frac{\rho_1}{6} \sum_{i=1}^{N} [(x_i - x_{i+1})(y_i^2 + y_i y_{i+1} + y_{i+1}^2)] \\ & + \frac{\rho_2 - \rho_1}{6} \sum_{i=1}^{N} [(\hat{x}_i - \hat{x}_{i+1})(\hat{y}_i^2 + \hat{y}_i \hat{y}_{i+1} + \hat{y}_{i+1}^2)] \\ A \quad = \quad & \frac{\rho_1}{2} \sum_{i=1}^{N} (y_i + y_{i+1})(x_i - x_{i+1}) + \frac{\rho_2 - \rho_1}{2} \sum_{i=1}^{N} (\hat{y}_i + \hat{y}_{i+1})(\hat{x}_i - \hat{x}_{i+1}). \end{aligned} \tag{6}$$

Here (x_i, y_i) and $(\hat{x}_i, \hat{y}_i)$ are the coordinates of the nodes on the membrane and nucleus respectively, ρ_1 is the density of the cytoplasm and ρ_2 is the density of the nucleus. We note that it is possible to use the relative densities of the cytoplasm and nucleus in (6) instead of the density.

2.4. Concentration gradient

In Chen et al. (2018) the concentration of the chemical signal was modelled by a time-dependent Poisson type equation. In reality, the concentration of the chemical signal will spread out from its source location and decay over time. Such processes can be modelled using the linear diffusion equation

$$\frac{\partial c}{\partial t} = \mu \left(\frac{\partial^2 c}{\partial x^2} + \frac{\partial^2 c}{\partial y^2} \right) \tag{7}$$

where c is the concentration of the chemical signal and $\mu > 0$ is the diffusion constant. It is straight-forward to show that the solution to the differential equation (7) due to a point source located at (x_s, y_s) is

$$c(t, \mathbf{x}_i(t)) = \frac{A}{\mu(t + t_\epsilon)} \exp\left(-\frac{(x(t) - x_s)^2 + (y(t) - y_s)^2}{4\mu(t + t_\epsilon)} \right) \tag{8}$$

where $t_\epsilon = 1 \times 10^{-6}$ is a small parameter to avoid computational problems when $t = 0$, and A is the source intensity. The source intensity controls the size of the chemical signal secreted by the cell and the diffusion constant controls how quickly the signal spreads out from the source.

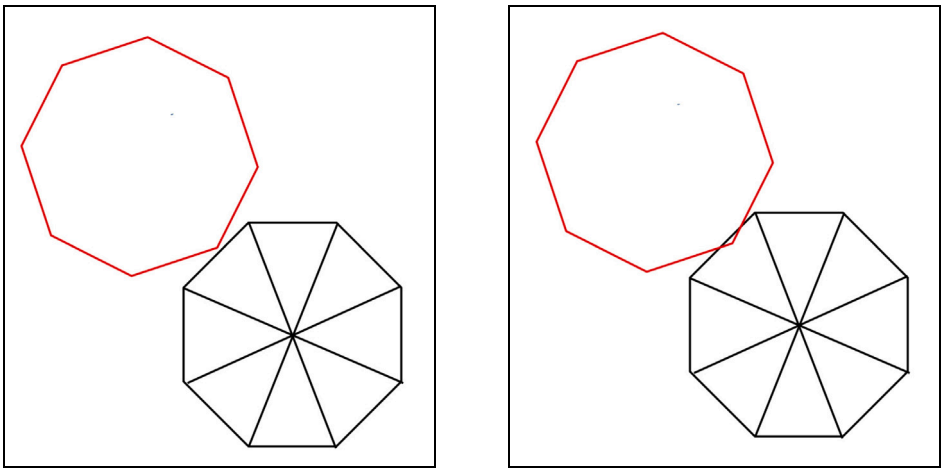

Fig. 3. During a collision one (or more) nodes on the membrane of one cell (shown in red) will pass into one of the triangles formed by each pair of nodes on the membrane and centroid of a second cell (shown in black).

The gradient of the concentrations, required in (4), can be found by simply differentiating (8) to give

$$\begin{aligned}\frac{\partial c}{\partial x} &= -\frac{A(x-x_s)}{2\mu^2(t+t_\epsilon)^2}\exp\left(-\frac{(x(t)-x_s)^2+(y(t)-y_s)^2}{4\mu(t+t_\epsilon)}\right)\\ \frac{\partial c}{\partial y} &= -\frac{A(y-y_s)}{2\mu^2(t+t_\epsilon)^2}\exp\left(-\frac{(x(t)-x_s)^2+(y(t)-y_s)^2}{4\mu(t+t_\epsilon)}\right).\end{aligned} \tag{9}$$

Although it is possible for the source point to be any point in the fluid, the signal is often secreted by one (or more) of the cells to attract other nearby cells. To simulate such problems, the source point is chosen to be at the centre of mass of one of the cells. Further, it is possible to define sources at the centre of more than one of the cells, and that each cell can start secreting the signal at different times. If a cell starts secreting the chemical signal when $t = t_0$ instead of when $t = 0$ then (8) can be modified to give

$$c(t,\mathbf{x}_i(t)) = \begin{cases} \dfrac{A}{\mu(t-t_0+t_\epsilon)}\exp\left(-\dfrac{(x(t)-x_s)^2+(y(t)-y_s)^2}{4\mu(t-t_0+t_\epsilon)}\right) & t \geq t_0 \\ 0 & t < t_0 \end{cases}.$$

2.5. Detecting cell collisions and cell clustering

To model collisions, we need to detect when a node on cell A has moved inside of cell B, as illustrated in Fig. 3 where cell A is shown in red and cell B (which has been divided into triangles) is shown in black.

Let the coordinates of the centroid of cell B be (x_1, y_1) and let (x_2, y_2) and (x_3, y_3) be the coordinates of two adjacent nodes on the membrane of cell B. Further let (x_a, y_a) be the coordinates of one of the nodes on the membrane of cell A. Solve the equations

$$\begin{aligned} x_a &= (1-u-v)x_1 + ux_2 + vx_3 \\ y_a &= (1-u-v)y_1 + uy_2 + vy_3 \end{aligned}$$

for u and v. If $u > 0$, $v > 0$ and $u+v < 1$ then (x_a, y_a) is inside the triangle formed from cell B and hence the two cells have collided but if at least one of the three conditions on u and v is not satisfied then the node on cell A has not collided with the triangle on cell B. This procedure is repeated for each node on the membrane of cell A and each triangle in cell B. If at least one node on cell A is inside a triangle of cell B then the two cells have collided. If a collision is detected for a particular triangle in cell B, then the nodal point on cell A will lock on to the closest of either (x_2, y_2) or (x_3, y_3). If N is small, then this may be noticeable, as the distance between two nodal points is visible, however the larger the value of N, the more negligible this becomes.

Suppose that the ith node from cell A needs to be combined with the jth node from cell B. The single combined equation for both nodes is (where subscripts i and j refer to nodes on the membrane of the appropriate cell and the superscripts denote which cell the nodes are on)

$$\begin{aligned} d\mathbf{m}_i(t) = {} & \beta\nabla c(t,\mathbf{m}_i^A(t))\,dt + \alpha(\mathbf{n}_i^A(t) - \mathbf{m}_i^A(t) - \mathbf{x}_i^A)\,dt \\ & - \delta(\mathbf{m}_i^A(t) - \mathbf{m}_{i+1}^A(t) - \mathbf{y}_i^A)\,dt + \delta(\mathbf{m}_{i-1}^A(t) - \mathbf{m}_i^A(t) - \mathbf{y}_{i-1}^A)\,dt \\ & + \alpha(\mathbf{n}_j^B(t) - \mathbf{m}_j^B(t) - \mathbf{y}_j^B)\,dt - \delta(\mathbf{m}_j^B(t) - \mathbf{m}_{j+1}^B(t) - \mathbf{x}_j^B)\,dt \\ & + \delta(\mathbf{m}_{j-1}^B(t) - \mathbf{m}_j^B(t) - \mathbf{y}_{j-1})\,dt \end{aligned} \tag{10}$$

When two cells collide, they form a common boundary or edge between them which is no longer in direct contact with the surrounding fluid. This means that the rate at which the cell reacts to the chemical signal or its gradient will be reduced. This is incorporated into the model presented here by reducing the value of β at all the nodes on the cells membrane by a factor of $k^{n_{c,i}}$ where $k \in (0, 1]$ is a constant which we will refer to as the reaction damping factor, and $n_{c,i}$ is the number of nodes on the membrane of the i^{th} cell that are attached to the nodes of a different cell. In the results presented here $k = 0.2^{1/100} = 0.9840344433646$ is used as this means β is reduced to 20% of its original value when 100 nodes on the cell's membrane are in contact with nodes on the membrane of another cell.

2.6. Time-stepping methods

Eqs. (4) (or (10) if two or more cells have collided) and (5) form a system of ordinary differential equations which we can solve for the locations of the nodes on the cell membranes and nuclei. However, the equations are too complex to solve analytically and so have to be solved numerically.

Consider the general first order ordinary differential equation

$$\frac{dy}{dt} = f(t, y(t))$$

subject to the initial condition $y = y_0$ when $t = 0$. If y_n denotes the approximate solution at time $t = nh$ where h is the time-step, then the method used here is

$$y_{n+1} = \frac{4}{3}y_n - \frac{1}{3}y_{n-1} + \frac{2h}{3}f(nh, y_n), \qquad n = 1, 2, \ldots \tag{11}$$

where Euler's method

$$y_1 = y_0 + hf(0, y_0)$$

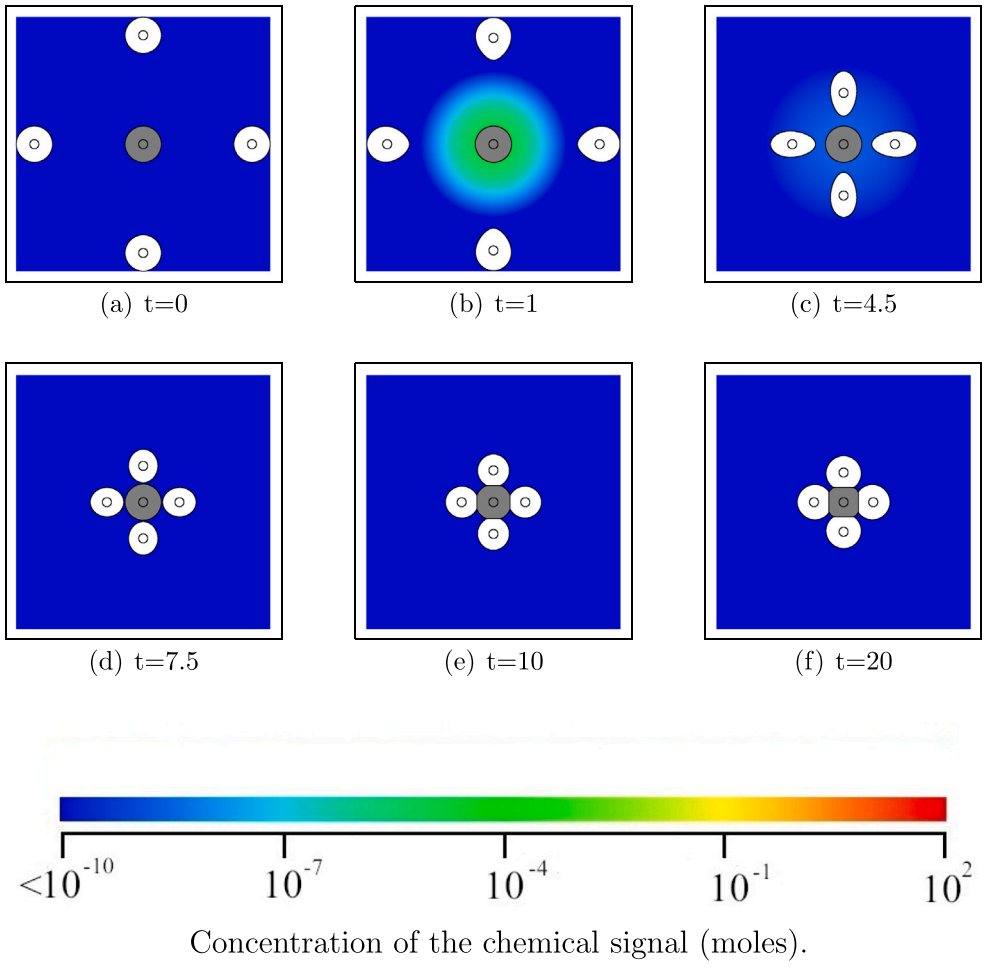

Fig. 4. The motion of 4 cells placed equidistant and symmetrically about a central cell (coloured grey) which is emitting the signal. All times are given in hours. The results shown in this figure show that the motion has the expected symmetry. This shows that the method is reproducing the expected motion. All times are given in hours.

is used to compute the first time-step as y_{-1} is not available. At each time-step, the above numerical scheme (11) is applied to each node on the membrane and nucleus in turn to update the location of the cell. Once the updated locations of the membrane and nucleus have been found the method described in Section 2.3 are used to update **c** the location of the centre of mass of the cell.

2.7. Parameters

The parameters used in this paper are summarised in Table 1.

In the literature the radii of cells used in numerical simulations range from 7 μm in Stonko et al. (2015) to 12.5 μm in Chen et al. (2018), Sfakianakis et al. (2018). Since the model presented here is general and not applied to one particular type of cell, the lengths are expressed in terms of cell radii. Values for the relative density of cytoplasm given in the literature range from 1 (Moran et al., 2010) to 1.3 (Kim and Guck, 2020) whilst the corresponding values for the nucleus is 1.4 (Kim and Guck, 2020).

The times are given in hours as the cells move very slowly.

Typically a cell will secrete a very small amount of the protein that is the chemical signal and hence the magnitude of the chemical signal is measured in moles. The parameter A in the solution to the diffusion equation, given by Eq. (8), is the source intensity and is the mass of chemical signal emitted by the cell. If A is chosen to be too large then the concentration of the chemical signal can overwhelm the receptors in adjacent cells and cause them to move unrealistically fast. On the other hand, if A is chosen to be too small, by the time the chemical signal reaches another cell its concentration is too small to have a significant effect on that cell. The choice $A = 15$ moles is consistent with the value of the secretion rate (1.2×10^{-6} mole/hour/(μm)^3) used in Chen et al. (2018) after the differences due to the diffusion equation model and the different units for distances used here are taken into account.

Table 1
The values of the parameters used in the calculations presented in this paper.

Parameter	Symbol	Values	Unit
Number of nodal points	N	500	
Radius of membrane		1	cell radii
Radius of nucleus		0.25	cell radii
Cell internal deformation relaxation coefficient	α	0.5	per hour
Cell membranes deformation relaxation coefficient	δ	30.0	per hour
Cell nucleus deformation relaxation coefficient	α_n	100.0	per hour
Cell response to external signal	β	2.5	per mole
Relative density of cytoplasm	ρ_1	1.2	
Relative density of nucleus	ρ_2	1.4	
Diffusion constant	μ	2.0	(cell radii)^2/hour
Source intensity	A	15.0	mole
Number of time-steps	n	10,000	
Maximum time		20	hours

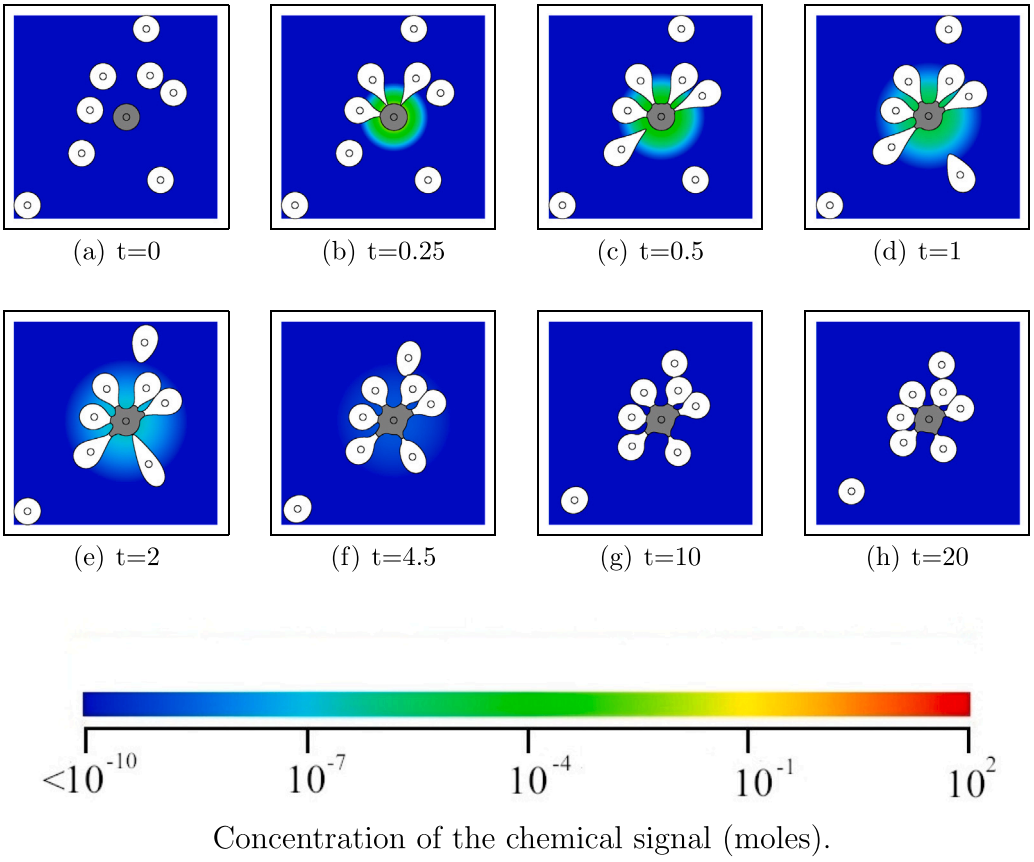

Fig. 5. The motion of 8 cells placed randomly about a central cell (coloured grey) which is emitting the signal. This example shows that cells closer to the emitting cell arrive first and that cells further away are slower to respond and may not reach the emitting cell. All times are given in hours.

The value of the diffusion parameter μ controls how quickly the chemical signal spreads out from an emitting cell. If the value of μ is too small then the chemical signal will take a long time to spread out from the emitting cell and so the time that it takes for the cells to react to the chemical signal is too long. However, if the value of μ is too large the chemical signal will spread too quickly and decay to close to zero before the cells have had time to react to the signal. Harris (2017) used a simple particle model to explore how different values of the diffusion parameter μ affects the rate at which the chemical signal spreads out from the cells emitting the signal and hence how rapidly the other cells are attracted to the emitting cells to form clusters. The results in Harris (2017) indicate the using values of μ between 1 and 10 (cell radii)^2/hour produce realistic results so the value $\mu = 2$ (cell-radii)^2/hour was used to obtain the results presented in this paper.

The relaxation parameters are derived from those in Chen et al. (2018) and have been rescaled due to the different units that we have used for lengths. The membrane relaxation parameter, which does not appear in the model presented in Chen et al. (2018), was chosen to be one which accurately simulated an isolated cell returning to its original shape when its motion stopped due to the chemical signal decaying to the level where its effect is small enough to be negligible.

The parameters used in this paper were chosen to give realistic looking simulations. A possible method for extending this model to match the motion of real cells captured using time lapse photograph or video is considered in the Discussion Section (Section 4).

3. Results

In this section we present the results of simulating the motion of circular cells in some different configurations. It is worth noting at this point that the cells do not have to be circular and that the methods discussed in Section 2 can be applied to cells with membranes and/or nuclei which have other shapes, albeit with the minor restriction that the boundaries should be convex in shape.

In all the figures below, the cells emitting the signal are coloured grey and the other cells are coloured white. In both cases the outer black curve is the cell membrane and the inner curve is the boundary of cells the nucleus. The colouring outside of the cells shows the concentration of the chemical signal in the surrounding medium, as given by Eq. (8), and is displayed on a logarithmic scale.

In the first example, shown in Fig. 4, there are four cells placed symmetrically above, below, to the left and to the right of a fifth central cell that is emitting the chemical signal. The outer cells are initially 6 cell radii from the central cell. As the motion of the cells changes over time we display the results at non-equal time steps to show the most important features of the cell motion. This is because the majority of the drastic movement happens within the first few hours of our 20 h interval before the chemical signal from the emitting cell decays away.

In this example, we would expect the motion of the four outer cells to have the same symmetry as the original cells, and that the central cell will not move. The results presented in Fig. 4 show that the motion of the four cells do have the expected symmetry, and this gives us some confidence that our numerical method is performing as expected. In addition, the motion of the central cell is smaller than the expected error in the numerical method used, and so can be considered to be zero to within the precision of the numerical methods that are being used.

The results shown in Fig. 5 show a group of 8 cells that have been randomly placed about a single emitting cell where a random number generator has been used to compute the coordinates of the cells with the only condition being that they are not allowed to overlap at the start. As expected, the cells that are closest to the emitting cell arrive at the

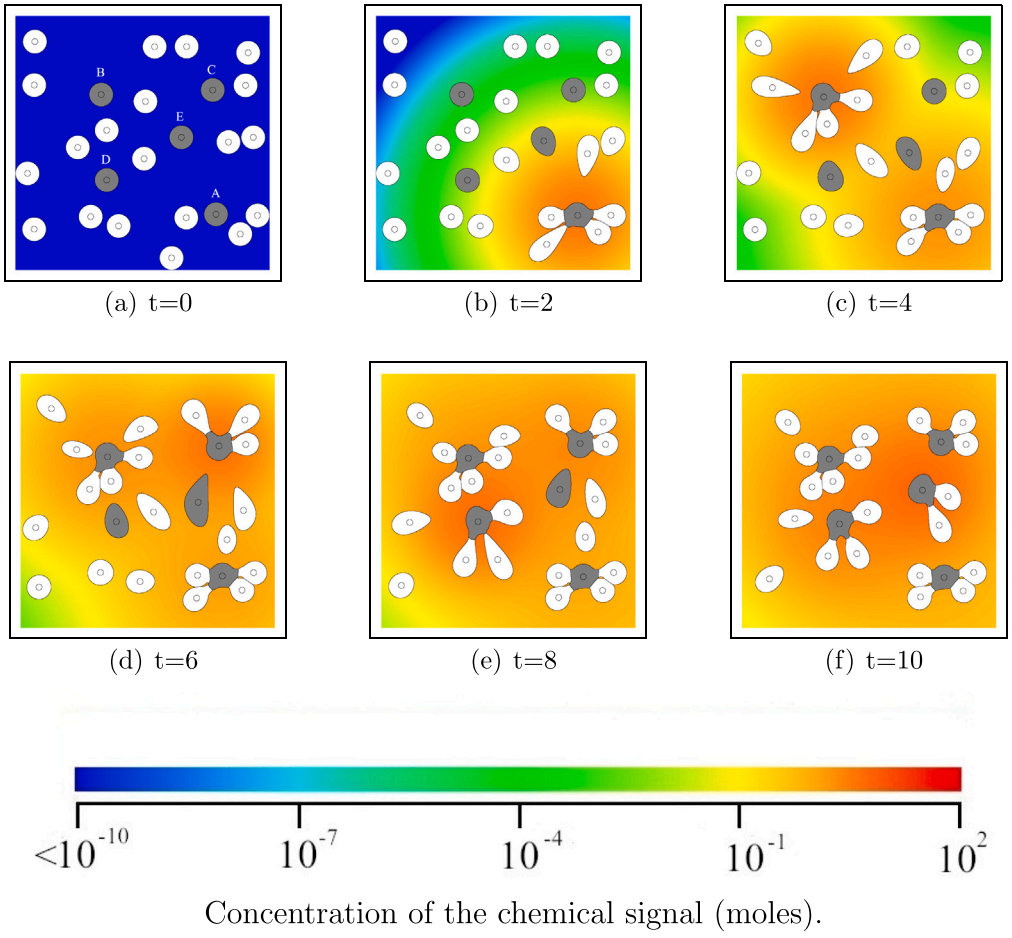

Fig. 6. The motion of 25 cells where 5 of the cells (coloured grey) emit the chemical signal. Times at which the cells start emitting the signal are $t = 0, 2, 4, 6$ and 8 for the cells labelled A, B, C, D and E respectively in the time $t = 0$ frame. All times are given in hours.

emitting cell first. In addition, the parts of the membranes of those cells that are closest to the emitting cell get stretched towards to emitting cell as the gradient in the chemical signal is larger on the sides of the cells closest to the emitting cell. This can be seen in Figs. 5(b)–(d).

This example also shows that the cells that are further away either attach to the outside of the cluster, such as the cell that starts at the top in Fig. 5, or do not reach the cluster at all, such as the cell which starts at the bottom left corner in Fig. 5.

Fig. 6 shows the results for 25 randomly positioned cells where 5 of the cells (shown in grey) are able to emit the chemical signal and each starts emitting the signal at a different time. The emitting cells are labelled A, B, C, D and E in Fig. 6(a) and they start emitting the chemical signal at times $t = 0, 2, 4, 6$ and 8 respectively. Fig. 6(b) shows that up until time $t = 2$ (which is when Cell B starts to emit the chemical signal) the cells are attracted towards Cell A as this the only cell producing a signal up until this time, and that the cells closer to Cell A are attracted more than those further away. The subsequent Figs. 6(c)–6(f) show how the cells are attracted towards the other emitting cells after they have started producing a signal. Fig. 6(c) shows how the non-emitting cell located between emitting Cells D and E forms an elongated shape as it attracted towards the signals produced by both Cells A and B.

4. Discussion and conclusions

This paper has presented a new mathematical model of how individual cells can come together by chemotaxis and join to form clusters. The model can be used to simulate different numbers of cells, different numbers of cells emitting the chemical signal and at different times, as illustrated by the examples shown in Figs. 5 and 6. Further, the number of cells that can be simulated by this model is only limited by the computational resources available. The memory requirements for the method presented here are quite small as the model of a typical cell with 500 nodes on both its membrane and nucleus will require less than 0.25Mb of memory. However, the CPU time needed is more of a issue. The calculations for the examples given in Figs. 4–6 required approximately 12, 50 and 480 min of CPU time respectively on a Windows 10 PC equipped with a Ryzen9 5900x processor running at 4.8 GHz and using gfortan code to carry out the calculations. The most expensive stage of the calculations is detecting the collisions, since when there are N cells with n nodes on the membrane of each cell then the CPU time for checking for a collision is approximately proportional to $(nN)^2$. The other stages of the calculations are approximately proportional to nN where the main cost is in calculating the nodal interactions. The computational cost of evaluating (9) for the gradient of the chemical signal at each node point on the membranes of the cells is relatively small.

The model presented here (and in Chen et al., 2018) are more efficient, from a computational point of view, than models which use methods like the finite element method, such as the one presented in Elliott et al. (2012). The finite element method will require the formation and solution of a system of algebraic equations at each time-step as well as a scheme to integrate the equations through time, whereas the spring-based model presented here only requires a time-stepping scheme to integrate the governing equations. Hence a model which uses the finite element method will require significantly more CPU

time and computer memory than the spring-based model presented here. Further, the computational cost of a model which uses the finite element method will be significantly more when it is used to simulate the motion of more than one cell.

Previous mathematical models of how cells migrate to form clusters have only considered very simple scenarios, such as the one proposed by Harris (2017) which treats the cells as rigid particles, whereas the model proposed here also simulates how the cells change shape in the course of their motion. Other models, such as the one developed by Chen et al. (2018), have simulated how cells move in response to a chemical signal, but have not simulated how cells collide and join together to form clusters. The model presented here extends the model developed by Chen et al. (2018) to include cell collisions and adhesions and so can simulate the shapes of cells after they have collided unlike the models which treat the cells as rigid particles. The shapes of the cells as they form clusters obtained using this model are very similar to those observed in experimental work, see Fig. 1 for example.

One possible extension of the model presented here is to use it estimate some of the parameters (such as the source intensity, diffusion constant, the reaction damping factor and the various relaxation coefficients) by minimising the difference between the locations and shapes of the cells observed in a time lapse video and the locations and shapes calculated using this model.

CRediT authorship contribution statement

Adam Farmer: Research in the paper, Discussion, Decided the results to include in the paper. **Paul J. Harris:** Supervision, Discussion, Decided the results to include in the paper.

Declaration of competing interest

The authors declare that they have no known competing financial interests or personal relationships that could have appeared to influence the work reported in this paper.

Acknowledgement

The authors would like to thank Matteo Santin from the Brighton Centre for Regenerative Medicine and Devices for his help and advice with the biological aspects of this work. They would also like to thank Manolia Andredaki for her help and advice with this research.

References

Alvarez-Elizondo, M.B., Merkher, Y., Shleifer, G., Gashri, C., Weihs, D., 2021. Actin as a target to reduce cell invasiveness in initial stages of metastasis. Ann. Biomed. Eng. 49, 1342–1352.

Ben-David, Y., Weihs, D., 2021. Modeling force application configurations and morphologies required for cancer cell invasion. Biomech. Model. Mechanobiol. 20, 1187–1194.

Chen, J., Weihs, D., Van Dijk, M., Vermolen, F.J., 2018. A phenomenological model for cell and nucleus deformation during cancer metastasis. Biomech. Model. Mechanobiol. 17 (5), 1429–1450.

Elliott, C.M., Stinner, B., Venkataraman, C., 2012. Modelling cell motility and chemotaxis with evolving surface finite elements. J. R. Soc. Interface 9, 3027–3044.

Eyiyurekli, M., Manley, P., Lelkes, P.I., Breen, D.E., 2008. A computational model of chemotaxis-based cell aggregation. BioSysytems 93, 226–239.

Harris, P.J., 2017. A simple mathematical model of cell clustering by chemotaxis. Math. Biosci. 294 (May), 62–70.

Hervas-Raluy, S., Garcia-Aznar, J.M., Gomez-Benito, M.J., 2019. Modelling actin polymerization: the effect on confined cell migration. Biomech. Model. Mechanobiol. 18, 1177–1187.

Kim, K., Guck, J., 2020. The relative densities of cytoplasm and nuclear compartments are robust against strong perturbation. Biophys. J. 119, 1946–1957.

Kim, M., Reed, D., Rejniak, K.A., 2014. The formation of tight tumor clusters affects the efficacy of cell cycle inhibitors: A hybrid model study. J. Theoret. Biol. 352, 31–50.

Löbor, J., Ziebert, F., Aranson, I.S., 2015. Collisions of deformable cells lead to collective migration. Sci. Rep. 5.

Massalha, S., Weihs, D., 2017. Metastatic breast cancer cells adhere strongly on varying stiffness substrates, initially without adjusting their morphology. Biomech. Model. Mechanobiol. 16 (3), 961–970.

Moran, U., Phillips, R., Milo, R., 2010. Snapshot: key numbers in biology. Cell 141.

Mousavi, S.J., Doweidar, M.H., 2015. Three-dimensional numerical model of cell morphology during migration in multi-signaling substrates. PLoS ONE 10.

Nitta, N., Tsuchiya, T., Yamauchi, A., Tamatani, T., Kanegasaki, S., 2007. Quantitative analysis of eosinophil chemotaxis tracked using a novel optical device — Taxiscan. J. Immunol. Methods 320, 155–163.

Peng, Q., Vermolen, F., 2020. Agent-based modelling and parameter sensitivity analysis with a finite-element method for skin contraction. Biomech. Model. Mechanobiol. 19, 2525–2551.

Sfakianakis, N., Peurichard, D., Brunk, A., Schmeiser, C., 2018. Modelling cell–cell collision and adhesion with the filament based lamellipodium model. Biomath 7.

Stonko, D.P., Manning, L., Starz-Gaiano, M., Peercy, B.E., 2015. A mathematical model of collective cell migration in a three-dimensional heterogeneous environment. PLoS ONE 10 (4).

Thompson, R.N., Yates, C.A., Baker, R.E., 2012. Modelling cell migration and adhesion during development. Bull. Math. Biol. 74, 2793–2809.

Vermolen, F.J., 2015. Particle methods to solve modelling problems in wound healing and tumor growth. Comput. Part. Mech. 2, 381–399.